

Implications of the Second Generation Intact Stability Criteria When Applied to A NZ off shore Patrol Vessel

Bryden Reay¹, Hossein Enshaei²

^{1,2}National Centre Marine Engineering and Hydrodynamics, Australian Maritime College, Australia

ABSTRACT: To address the problems of dynamic stability failures, the International Maritime Organisation plan to supersede the intact stability criteria. The draft criteria have been applied to a New Zealand naval patrol vessel to aid in understanding the implication imposed by the revised criteria. This paper addresses how the criteria were applied to the vessel and presents the outcomes of the calculated vulnerabilities. A computational simulation was conducted for the broaching phenomenon using four possible phenomenon-inducing wavelengths. It was found that the patrol vessel broached by more than fifteen degrees over a seven second time period. Therefore, taking into account the simplifications of the analysis, the OPVs, like other vessels, could be deemed vulnerable to the surf-riding and broaching-to phenomenon for these given, operationally avoidable, encounter conditions. Further analysis is recommended when the draft criteria is finalised.

Keywords: Broaching-to, Computational Fluid Dynamics, Patrol Vessel, Second Generation Intact Stability Criteria, Surf-riding

I. INTRODUCTION

It has been observed that over the past 40 years' numerous stability related accidents have occurred, inducing the argument that the Intact Stability (IS) Criteria should be revised [1]. Some of these accidents have been investigated experimentally to determine why the vessel has capsized. Kure and Band [2] investigated the stability of a small tanker that was believed to have a varying GZ curve as the waves overtook her in stern quartering seas. It was discovered that this condition resulted in a continuous lagging in roll motion and subsequently induced a resonance, ultimately leading to the vessels capsize. Following on from this event, France [3] investigated the loss of a container ship through numerical simulations. The results indicated that the vessel was susceptible to head-sea parametric rolling with the amplitude predicted to be approximately 30 degrees. Numerical simulations conducted proved to be useful where it consistently showed that a ship had insufficient stability due to the pure loss of stability phenomenon when the wave crest was situated on amidships [4]. Rojas concluded that the current IS criteria was neither sufficient nor suitable for vessels operating in waves that alter the ships stability.

As a result, the IMO tasked a Sub-Committee to develop a means to determine the susceptibility of vessels. In response, a process of analysis was developed by the Sub-Committee on Stability and Load Lines and on Fishing Vessels' Safety (SLF) at SLF53 to detail how vessels will be assessed against the Second Generation Intact Stability Criteria (SGISC) failure modes. The SLF are now known as the IMO Sub-Committee on Ship Design and Construction (SDC) after the IMO restructured selected sub committees and disbanded the SLF. The process of analysis for the SGISC developed by the SLF is shown in Fig. 1. There are four failure modes not including excessive accelerations, which need to be taken into consideration at three different levels.

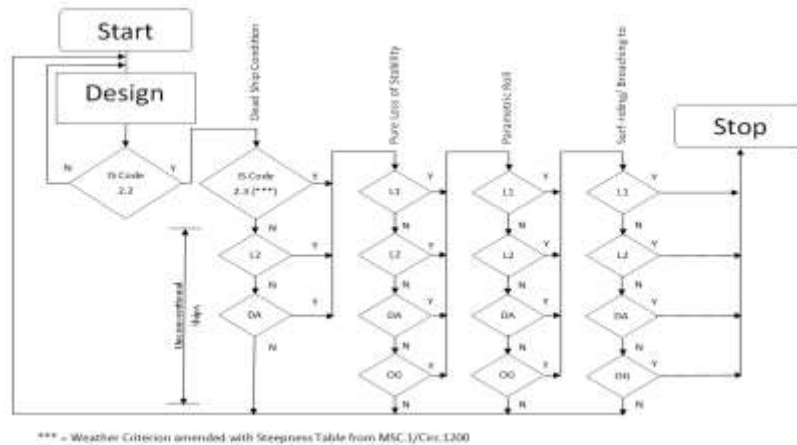


Fig. 1: SGISC Process of Analysis [5]

Deadship Condition

The first level of the SGISC for the Deadship condition is an amended version of the IMO Weather Criterion. The worst possible scenario will occur when the vessel is subjected to beam seas, combined with a gusty wind; thereby inducing a resonant roll [6]. A summary of the development to date can be sourced from SDC 1/INF.6.

Pure Loss of Stability

Peters [1] describes the pure loss of stability as an occurrence that originates from the geometric variances of the hull. Fig. 2a describes the variance of the GZ curve and shows how the righting moment will be higher when the wave trough is at amidships. As the wave crest is at amidships, the wave troughs are found at the fore and aft sections, thereby reducing the water plane area of the vessel and subsequently reducing the righting moment of the vessel as shown in Fig. 2b. The pure loss of stability phenomenon is most apparent when the wavelength is equal to the length of the vessel.

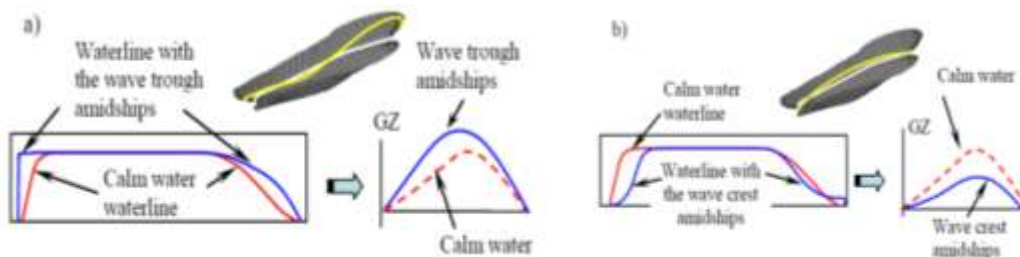


Fig. 2: a) Variance of Stability when Wave Trough is at Amidships and b) Variance of Stability when Wave Crest is at Amidships [7]

The probabilistic criteria developed for the pure loss of stability phenomenon can be found by referring to Belenky [7].

Parametric Roll

Parametric roll has been described as the gradual amplification of the roll amplitude produced by parametric resonance. Bassler [6] states that this is a consequence of periodic changes of the vessels stability in waves. As shown in Fig. 3 the GZ curve varies greatly depending on whether the wave crest or trough is situated amidships.

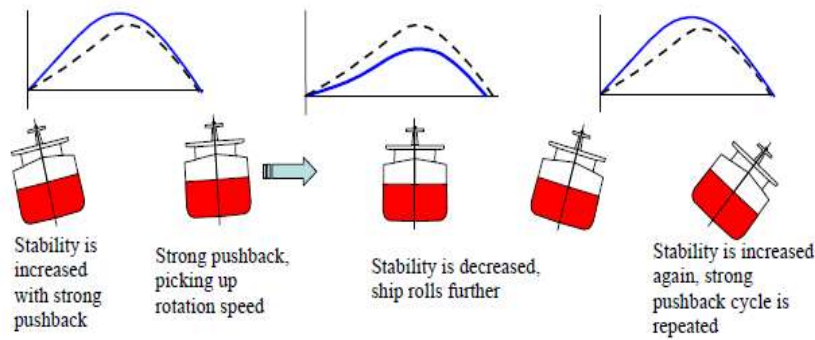


Fig. 3: Development of the Parametric Roll Phenomenon [7]

If the encounter frequency of the waves is equal to half of the roll frequency of the vessel, the roll amplitude may gradually increase, if roll damping does not combat the hysteresis energy gain, or course/speed changes are not made to the encounter conditions, as shown in Fig. 4. It has been determined over numerous experimental results that parametric roll occurs when the wave length is approximately equal to the waterline length of the vessel, usually $\lambda/L = 1.0 \pm 0.2$ [8][9][10].

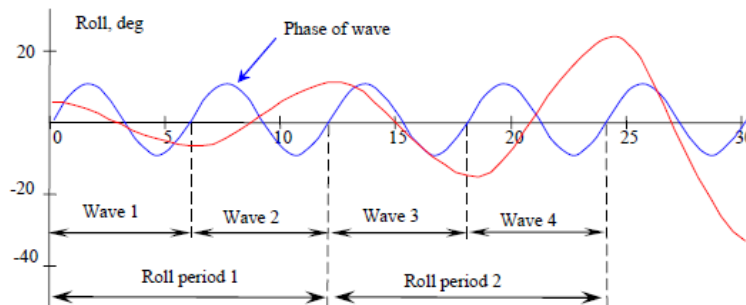


Fig. 4: The Encounter Frequency Relationship to Parametric Roll [7]

The first level, susceptibility criteria, was formulated upon changing GM in regular waves and the Mathieu equation. Detailed information is given in the American Bureau of Shipping (ABS) guide on assessment of parametric roll on container ships.

Surf-riding/Broaching-to

The surf-riding/ broaching-to criterion has been developed from the phase plane method, by comparing this phenomenon to that of a pendulum. The phase diagram of a pendulum shown in Fig. 5a is remarkably similar to that of the phase diagram for a vessel surf-riding shown in Fig.5b.

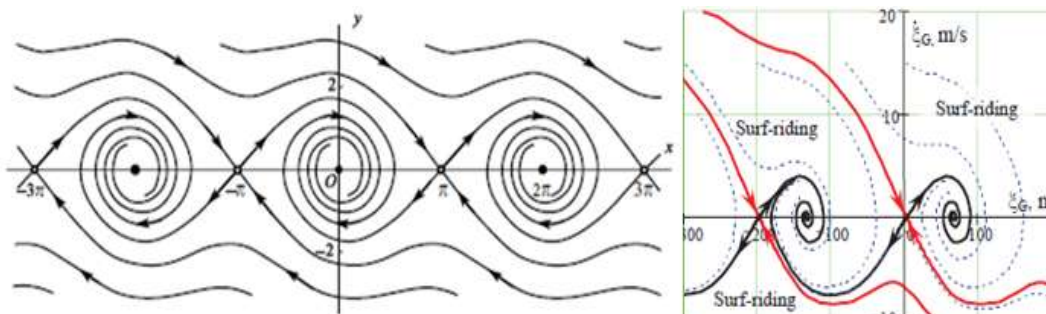


Fig. 5: a) Phase diagram for pendulum equation with small damping [11] and b) Phase plane with surf-riding at 24knots [12]

Mathematical model for surf-riding of a vessel subjected to regular following waves is provided by Belenky [12], and is as follows:

$$(m + m_x) \times \ddot{\xi}_G + R(c + \dot{\xi}_G) - T(c + \dot{\xi}_G, n) + F_w(\xi_G) = 0 \quad (1)$$

Where the Froude-Krylov force is the integration of the wave pressure over the surface of the hull [13] as shown:

$$F_w(\xi_G) = -\rho g k \zeta_A [A_s \sin(k\xi_G) - A_c \cos(k\xi_G)] \quad (2)$$

Surf-riding has been observed to occur when (1) is equal to zero, when the assumption that the velocity and acceleration of the ship relative to the wave celerity is also zero. Therefore:

$$R(c) - T(c, n) + F_w(\xi_G) = 0 \quad (3)$$

Along with the confirmation of pendulum consideration, analysis shows that the equilibrium near the wave crest is unstable, whereas in the wave trough is stable. As discussed by [7], for a particular speed surf-riding is only possible with the concurrence of surging. In non-linear dynamics it is known as the hetroclinic saddle connection, a type of bifurcation. The dynamics of the bifurcation has been identified and discussed by Spyrou [14]. This method of calculation has been determined to be excessively tedious; hence Melnikov's method is used to provide an approximate practical solution [15].

Excessive Accelerations

Excessive acceleration is another failure mode considered in SGISC. If a ship has excessive GM, the natural roll period becomes small. As a consequence, excessive accelerations could occur, which is intensified on the bridge of the vessel [16]. The derivation for the excessive accelerations criteria can be found by referring to Belenky [7]. This relationship can be seen from (4) and Fig. 6.

$$T = \frac{2 * C * B}{\sqrt{GM}} \quad (4)$$

Where:

$$C = 0.373 + 0.023(B / d) - 0.043(L_{WL} / 100) \quad (5)$$

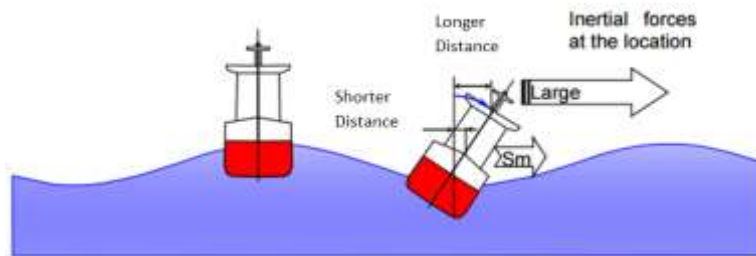


Fig. 6: Scenario of Stability Failure due to Excessive Accelerations

II. EXPERIMENTAL SETUP

The mathematical models were developed using the formulas prescribed by the Ship Design and Construction (SDC) Sub Committee for the SGISC. Many of the formulas required the application of external software such as Bentley Systems Maxsurf Suite. The simulations conducted include a large angle equilibrium analysis, to determine the righting lever characteristics for the Deadship condition; determining the hydrostatics of the subjected vessel for the pure loss of stability and parametric roll, a resistance test for the surf-riding/broaching-to phenomenon, and a roll decay simulation for the excessive accelerations. In addition, the wave cases required for parametric roll and pure loss of stability were computed prior to conducting simulations in Maxsurf. The projected lateral area for the Deadship condition and the projected bilge keel area used for the parametric roll criteria were both determined using a scale drawing of the vessels profile.

The resistance of the vessel was simulated by computational means, Ansys Cfx, and was verified using the Maxsurf Resistance results. The hull form used for the computational simulations is shown in Fig. 7. The fluid domain boundary dimensions, relative to the hull form, can be found in Table 1, with the image shown in Fig. 8.



Fig. 7: OPV Hullform Model

Table 1: CFX Resistance Simulation Fluid Domain Boundary Dimensions

Boundary	Dimensions (m)
Inlet	160
Outlet	240
Walls	80
Base and Ceiling	80

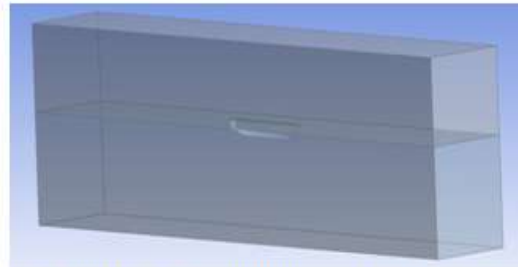


Fig. 8: Fluid Domain Configuration for the CFX Resistance Analysis on the OPV Hullform

The direct assessment simulations for the surf-riding/ broaching-to phenomenon were conducted using the Reynolds Averaged Navier Stokes (RANS) solver STAR-CCM+. The integral form of incompressible RANS equation is resolved using finite volume method of discretization in this software. Unsteady state RANS simulations were performed to investigate the hydrodynamic interaction forces and movements on the model scale vessel. A four Degrees of Freedom (DoF) transient setup using the Dynamic Fluid Body Interaction (DFBI) option. The boundary dimensions were reduced to the minimum recommended sizes stipulated by the ITTC and can be found in Table 2. A structured hexahedral mesh was generated based on recommendations for Dynamic Fluid Body Interaction (DFBI) simulations [17]. A time step of 0.01s was used for the simulations.

Table 2: Star CCM+ Broaching-to Simulation Fluid Domain Boundary Dimensions

Boundary	Dimensions (m)
Inlet	10
Outlet	10
Walls	10
Base and Ceiling	5

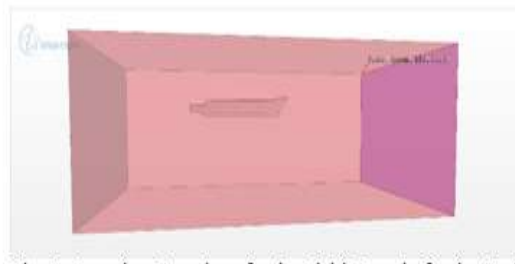


Fig. 9: Boundary Locations for the Fluid Domain for the Surf-Riding/ Broaching-to Simulation

Both CFD simulations were conducted using three dimensional Reynold Averaged Navier Stokes (RANS) equations. The Shear Stress Transport (SST), a combination of the K-epsilon and K-omega turbulence models, was utilised for the CFX simulation. The drawback of the SST model is that more computational time is required to complete the calculations; however, this was deemed permissible to ensure that the boundary layer effects were correctly calculated. The k-omega model is used in the inner region of the boundary layer and transitions to the k-epsilon in the free shear flow. K-epsilon doesn't perform well in large adverse pressure gradient and hence makes it not suitable for a ship simulation with prominent waves impacting and being generated by the vessel. K-omega on the other hand, has more difficulty converging than the other two models. In the Star CCM+ simulations the K-omega SST model was used.

III. LIMITATIONS AND ASSUMPTIONS

This section discusses the limitations of the assumptions employed to produce a result for the SGISC. The assumptions made in developing the criteria are mentioned in the references previously stated.

The Holtrop method was used for the resistance calculations. The Holtrop algorithm is designed for predicting the resistance of a range of ships including frigates and large patrol vessels [18]. The limitations of the Holtrop method were as follows:

$$\begin{aligned} 0.55 < C_p < 0.85 \\ 3.9 < L/B < 15 \end{aligned} \quad (6)$$

Where C_p is the prismatic coefficient. The vessel was found to be within both of these limitations.

The roll damping simulation did not take into account the bilge keels on the vessel due to the software having difficulties resolving appendages. To get a more accurate representation of the linear roll damping coefficient, a simulation would need to be conducted using Computation Fluid Dynamic (CFD) software. The underlying assumptions of linear strip theory also influence the result which include but are not limited to [19]:

- The fluid is inviscid, therefore viscous damping is ignored; and
- The presence of the hull has no effect on the waves, the Froude-Krylov hypothesis.

The moment of inertia (I) for the vessel is not supplied by Maxsurf motions. Therefore to calculate I_{xx} the following formula was required [20]:

$$I_{xx} = BM * \nabla \quad (7)$$

The roll period of the vessel was calculated as recommended by IMO [21], shown in (4). The SGISC called upon the height above the roll axis where personnel on-board could access. To simplify this, the distance from the roll axis to the centre of mass of the vessel was calculated using the empirical formula developed by Balcer [22].

$$b_w \approx 0.57 * (d - KG) - 0.1 * B \quad (8)$$

The wake fraction for the vessel was provided by the vessel owner, whereas the thrust deduction was determined by the following formula from Holtrop for twin screw vessels [23]:

$$t = 0.325 * C_B - 0.1885 * \frac{D}{\sqrt{B * d}} \quad (9)$$

The provisions for the pure loss of stability apply to all vessels over 24m with a Froude number corresponding to the service speed, which exceeds 0.24. The only provision required for the parametric roll and surf-riding phenomenon is that the vessel must have a length equal to or greater than 24m. For the provisions to apply for Excessive Accelerations, the highest location must be greater than 70% of the breadth, and the Metacentric Height of the vessel must be greater than 8% of the breadth.

The OPV propeller was assumed to be a Wageningen series propeller [23]. The Wageningen series have two to seven blades, a blade area ratio between 0.30 and 1.05 and pitch on diameter ratio between 0.60 and 1.40. Although the Wageningen series propellers are typically used in merchant vessels, it was deemed suitable for this application.

The CFX simulations neglect all the appendages of the hull form. John [24] states that approximately 15% additional resistance can be added for surface naval combatants operating at and above a Froude number of 0.3 to compensate for the appendages. The primary appendages are the rudders, propellers and bilge keels. The Star CCM+ simulations also neglect all the appendages of the hull form.

The first order waves are derived from linear wave theory. Therefore, the underlying assumptions are also applicable to the Star CCM+ simulation. The vessel is assumed to be operating in deep water. Therefore, it is assumed the model is operating in depths greater than 21m. RANS models the turbulence but does not fully resolve it. Therefore, the results will be more accurate if the turbulence of the vessel was fully solved.

The broaching-to simulation has not been validated by a model scaled vessel and therefore, there might be some uncertainty in the results of the broaching-to simulation.

IV. RESULTS AND DISCUSSION

Level One

Within the Deadship condition criterion, the wind heeling lever is calculated as a function of the centroid and projected lateral area. It can be seen from Fig. 10 that exposed area of the OPV is comparatively small, having a low centroid relative to the waterline. The bilge keels of the vessel are effective in reducing the heeling motion. The Deadship condition criterion has been applied to the GZ curve of the hull form as shown in Fig. 11. As per the criterion, the area b shall be equal or greater than area a. In Fig. 11 it can be seen that this is true. It should also be noted that the angle of equilibrium does not exceed 16° or 80% of the angle of deck edge

immersion; therefore, it passes all aspects of the criterion. The angle of down flooding was taken as the lesser of the angle at which water enters the first opening that cannot be closed, and 50 deg.



Fig. 10: Profile View of the OPV, HMNZS Wellington (image supplied)

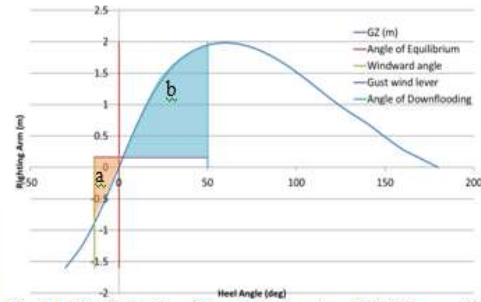


Fig. 11: Deadship Condition Righting Arm (GZ) Curve of the OPV

The vessel found to be vulnerable to the pure loss of stability phenomenon. The calculations showed that changes of draft (low) (δd_L) produce a large variation in the moment of inertia of the vessel which lead to the ships vulnerability. The variation of the draft is determined by the formula provided:

$$\delta d_L = \text{Min} \left(\left(d - 0.25d_{full} \right) \left(\frac{LS_w}{2} \right) \right) \quad (10)$$

The subjected vessel has a large L/d ratio with the operating draft very similar to the full draft. Therefore, it can be seen that:

$$\begin{aligned} d &\approx d_{full} \\ \therefore d - 0.25d_{full} &\approx 0.75d \end{aligned} \quad (11)$$

This in turn produces a large variance in the draft, ultimately resulting in the vessels vulnerability. The level one criterion was developed on the basis of analysing the variation of displaced volume of the fore and aft quarters; it does not take into account the trim and sinkage effects that a vessel would experience when traversing through large swells.

For parametric roll, the vessel found not to be vulnerable as per the criterion. The projected area of the bilge keels plays an important role in determining the vulnerability of the vessel. 35% reduction in the area of the bilge keels would make the vessel vulnerable for the level one criterion.

The vulnerability calculation for parametric roll is determined by a ratio of the variation of the metacentric height and the operating metacentric height. The results show that even though the variation of the metacentric height is significant for the hull form, it is nullified by the operating metacentric height. For the pure loss of stability, the criterion focuses only on the minimum metacentric height of the vessel.

The vessel was found to be vulnerable to the surf-riding/broaching-to phenomenon. Given the simplicity of the criteria, the only way to ensure a vessel is not vulnerable to surf-riding or broaching-to is to ensure that the vessel length is greater than 200m or to operate at a Froude number of less than 0.3.

The vessel also found not to be vulnerable to excessive accelerations. Once again, the projected area of the bilge keel has a great contribution in the vulnerability calculation; however, as mentioned in the Deadship condition criterion, the superstructure of the vessel is 22.5m above the waterline and therefore not significant in comparison to a vessel with immensely greater superstructure. Using the empirical formula derived by Balcer [22], the lateral acceleration was determined to be 4.58m/s; however, by using the assumption stated in the criteria, the lateral acceleration was determined to be 4.38m/s, a variation of 0.2m/s. When comparing the calculations, the distance from the roll axis changes from 19.95m to 18.68m. This is due to the assumption in the criterion that the roll axis is located at the midpoint between the waterline and the vertical centre of gravity.

Although the variations in the results are not significant, it is recommended that an appropriate empirical formula be used to determine the roll axis location. It is important to note that the excessive acceleration criterion does not take into account the vertical accelerations experienced, as the vessel operates in higher sea states. It only takes into account the motions illustrated in Fig. 6.

Level Two

The pure loss of stability level two criterion focuses on the righting arm (GZ) rather than the variation of the Moment of Inertia. Additionally, the criterion allows for the vessel to trim and sink freely. The bow of the vessel flairs out, as shown in Fig. 12 and the vessel also has a partially submerged transom. Therefore, when the vessel is permitted to trim and sink freely, the variation in GM is lessened significantly compared to the level one calculations for the pure loss of stability failure mode.

The surf-riding/broaching-to criterion is determined from the thrust and resistance information of the vessel. To calculate the thrust, the thrust potential from the propeller must be determined. This was completed using the Wageningen series [23], which is shown in Fig. 13. It was recommended by Haase [25] to determine the resistance from the required thrust of the vessel; however, it can be seen in Fig. 14 that the curve of thrust calculated resistance behaves differently after a Froude number of 0.4. To overcome this deficiency, a squared polynomial curve was used for the thrust calculated resistance, which is compared against the CFD results shown in Fig. 15.

The vessel speed used in the criteria is equal to the wave speed [26]. By knowing that the wavelength to vessel length ratio used in the criteria is a maximum of three and minimum of one, we can deduce the following:

$$Fn = \frac{c_w}{\sqrt{gL_{PP}}} = \frac{\sqrt{\frac{g\lambda}{2\pi}}}{\sqrt{gL_{PP}}} = \sqrt{\frac{\lambda/L_{PP}}{2\pi}} \tag{12}$$

$$\therefore Fn_{\lambda/L_{PP}=1} = \sqrt{\frac{1}{2\pi}} = 0.399; Fn_{\lambda/L_{PP}=3} = \sqrt{\frac{3}{2\pi}} = 0.691 \tag{13}$$

Therefore, the resistance curve must be valid up to a Froude number of 0.691 (37kts). However, the thrust calculated resistance is only valid up to a speed of 22.5kts (0.42).

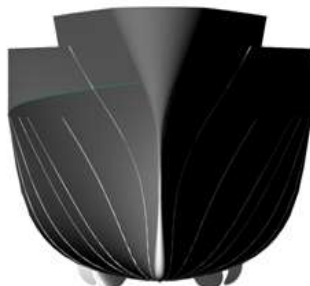


Fig. 12: Body Plan View of the OPV Model

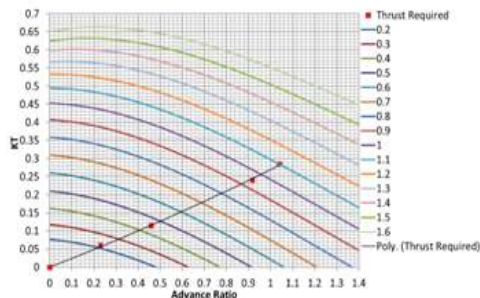


Fig. 13: KT-J Curve for the OPV Propeller

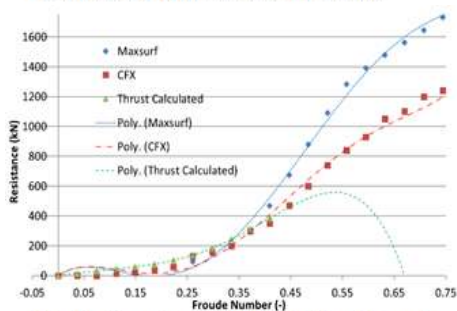


Fig. 14: Comparison of the Results from Maxsurf Resistance, CFX Simulation and the 5 Power Polynomial Thrust Calculated Resistance Results for the OPV

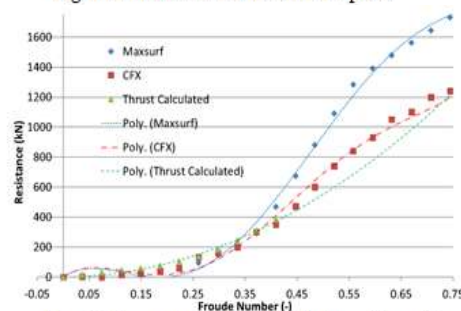


Fig. 15: Comparison of the Results from Maxsurf Resistance, CFX Simulation and the Squared Polynomial Thrust Calculated Resistance Results for the OPV

A discrepancy between the Maxsurf and CFX results is illustrated when plotting them in Fig. 15. Therefore, a 15% appendage allowance was added to the CFX resistance results to account for the appendages omitted from the analysis [24]. The modified results can be seen in Fig. 16.

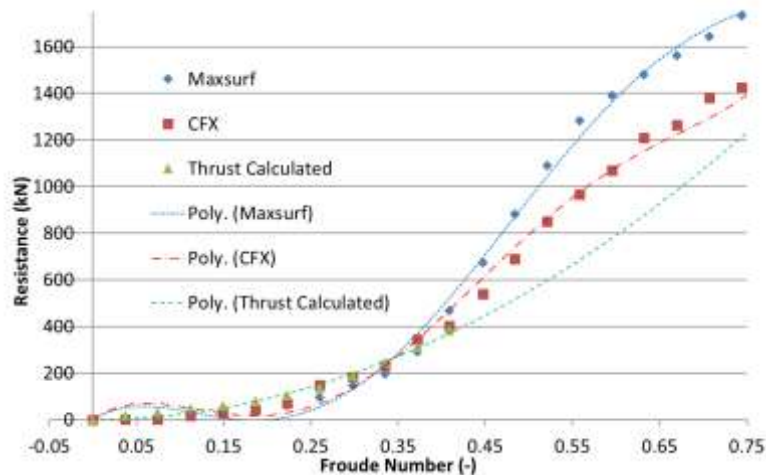


Fig. 16: Comparison of the Maxsurf Resistance Results and the CFX Simulation Results with Appendages Allowance for the OPV Hull Form

China [27] recommended to conduct a CFD simulation at only 3 speeds below a Froude number 0.4 due to the convergence errors that occur above 0.4. Noting however, that the resistance data required to determine the vulnerability for surf-riding/broaching-to is within the band width of Froude numbers 0.399 and 0.691. The recommendation by China [27] was adopted by extrapolating the CFX resistance data using a squared polynomial curve and comparing it to the CFX resistance within the bandwidth required. It was found that the squared polynomial curve under predicts the resistance of the vessel, as shown in Fig. 17. The relative error between the recommendation and the computationally determined results was found to be up to 30%.

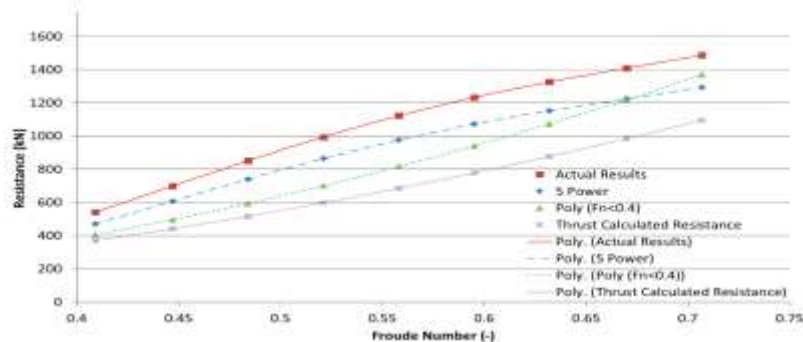


Fig. 17: Comparison of the Extrapolated Squared Polynomial Curve and the 5 Power Polynomial Curve Against the CFX Resistance Results with Appendage Correction

The resistance equation for the extrapolated squared polynomial curve is given at (14). The extrapolated squared polynomial curve as recommended by China [27] has a relative error that fluctuates between 8 and 30%. This approach is not recommended.

$$R = 3186.3V^2 - 315.36V \quad (14)$$

However, the 5 power polynomial curve introduces a constant error of 13%. The resistance equation for the 5 power polynomial curve is given at (15).

$$R = 95645V^5 - 196361V^4 + 136321V^3 - 33285V^2 + 2719.2V \quad (15)$$

This has an effect on the overall accuracy of the level two surf-riding/broaching-to results by under predicting the resistance. The 5 power polynomial curve has been used for the level two surf-riding/broaching-to program. For instances where the resistance of the hull form cannot be determined by Maxsurf, CFD or a similar program, the thrust calculated resistance equation can be used. The relative error is by far the largest out of the methods considered and fluctuates between 26% and 40%. The resistance equation for the thrust calculated resistance curve is given at (16).

$$R = 2162.2V^2 + 20.966V \quad (16)$$

The resistance and thrust curves of the OPV were used to determine the critical velocity by solving (17).

$$T_e(u_{cr}; n_{cr}) - R(u_{cr}) + f(r_i; s_j) = 0 \tag{17}$$

Table 3 contains the statistical weight of the waves investigated for the analysis. The waves contained within Table 3 were used to determine the vessels vulnerability weighting in (18) [5].

$$W_{ij} = \frac{4\sqrt{g}}{\pi\nu} \frac{L^2 T_{01}^5}{H_s^3} s_j^2 r_i^2 \left(\frac{\sqrt{1+\nu^2}}{1+\sqrt{1+\nu^2}} \right) \delta r^* \delta s^* \exp \left[-2 \left(L^* r_i^* \frac{s_j}{H_s} \right)^2 \left\{ 1 + \frac{1}{\nu^2} \left(1 - \sqrt{\frac{g T_{01}^2}{2\pi r_i L}} \right)^2 \right\} \right] \tag{18}$$

$$\text{Where, } \nu = 0.4256 = \sqrt{\frac{m_0 m_2}{m_1^2} - 1}$$

Table 3: Wave Case Occurrences per 100,000 Observations [5]

H _i (m)	T _r (s) = average zero-up crossing wave period															
	3.5	4.5	5.5	6.5	7.5	8.5	9.5	10.5	11.5	12.5	13.5	14.5	15.5	16.5	17.5	18.5
0.5	1.3	133.7	865.6	1186.0	634.2	186.3	36.9	5.6	0.7	0.1	0.0	0.0	0.0	0.0	0.0	0.0
1.5	0.0	29.3	986.0	4976.0	7738.0	5569.7	2375.7	703.5	160.7	30.5	5.1	0.8	0.1	0.0	0.0	0.0
2.5	0.0	1.2	197.5	2158.8	6230.0	7449.5	4860.4	2066.0	644.5	160.2	33.7	6.3	1.1	0.2	0.0	0.0
3.5	0.0	0.2	34.5	695.5	3226.5	5675.0	5099.1	2838.0	1114.1	337.7	84.3	18.2	3.5	0.6	0.1	0.0
4.5	0.0	0.0	6.0	196.1	1354.3	3288.5	3857.5	2685.5	1275.2	455.1	130.9	31.9	6.9	1.3	0.2	0.0
5.5	0.0	0.0	1.0	51.0	498.4	1602.9	2372.7	2008.3	1126.0	463.6	150.9	41.0	9.7	2.1	0.4	0.1
6.5	0.0	0.0	0.2	12.6	167.0	690.3	1257.9	1268.6	825.9	386.8	140.8	42.2	10.9	2.5	0.5	0.1
7.5	0.0	0.0	0.0	3.0	52.1	270.1	594.4	703.2	524.9	276.7	111.7	36.7	10.2	2.5	0.6	0.1
8.5	0.0	0.0	0.0	0.7	15.4	97.9	255.9	350.6	296.9	174.6	77.6	27.7	8.4	2.2	0.5	0.1
9.5	0.0	0.0	0.0	0.2	4.3	33.2	101.9	159.9	152.2	99.2	48.3	18.7	6.1	1.7	0.4	0.1
10.5	0.0	0.0	0.0	0.0	1.2	10.7	37.9	67.5	71.7	51.5	27.3	11.4	4.0	1.2	0.3	0.1
11.5	0.0	0.0	0.0	0.0	0.3	3.3	13.3	26.6	31.4	24.7	14.2	6.4	2.4	0.7	0.2	0.1
12.5	0.0	0.0	0.0	0.0	0.1	1.0	4.4	9.9	12.8	11.0	6.8	3.3	1.3	0.4	0.1	0.0
13.5	0.0	0.0	0.0	0.0	0.0	0.3	1.4	3.5	5.0	4.6	3.1	1.6	0.7	0.2	0.1	0.0
14.5	0.0	0.0	0.0	0.0	0.0	0.1	0.4	1.2	1.8	1.8	1.3	0.7	0.3	0.1	0.0	0.0
15.5	0.0	0.0	0.0	0.0	0.0	0.0	0.1	0.4	0.6	0.7	0.5	0.3	0.1	0.1	0.0	0.0
16.5	0.0	0.0	0.0	0.0	0.0	0.0	0.0	0.1	0.2	0.2	0.2	0.1	0.1	0.0	0.0	0.0

Direct Assessment

The simulations were completed in accordance with the ITTC CFD recommendations [28]. The model vessel has been defined as a four DoF body, where surge and sway were restrained. Because the hull form was constrained in surge, the velocity of the hull form could not increase; this would have an affected the vessel’s directional stability. Although this does not portray the true characteristics of a hull form’s behaviour but, it allows the surf-riding and broaching-to characteristics to be separated for investigation on an individual basis. Due to time restraints, only the broaching-to characteristics were investigated and reported on.

The waves generated in the simulation are first order waves using the Volume Of Fluid (VOF) method, where the VOF method is used to model a free surface. The wavelengths of interest, between one and three times the vessels length, were identified on the global wave scatter diagram as shown in Table 4. From the global wave scatter diagram, Table 4, a wave height of 3.5m has been chosen. The wave height and wavelengths were scaled to a model scale and the wave lengths simulated are displayed in Table 5. The scaled wave height was determined to be 0.211m.

Table 4: Global Wave Scatter Diagram with Applicable Waves Identified

Significant Wave Height H _s (m)	Wavelength (m)					
	87.82	112.8	140.91	172.13	206.48	243.95
0.5	0.6%	0.2%	0.0%	0.0%	0.0%	0.0%
1.5	7.7%	5.6%	2.4%	0.7%	0.2%	0.0%
2.5	6.2%	7.4%	4.9%	2.1%	0.6%	0.2%
3.5	3.2%	5.7%	5.1%	2.8%	1.1%	0.3%
4.5	1.4%	3.3%	3.9%	2.7%	1.3%	0.5%
5.5	0.5%	1.6%	2.4%	2.0%	1.1%	0.5%
6.5	0.2%	0.7%	1.3%	1.3%	0.8%	0.4%
7.5	0.1%	0.3%	0.6%	0.7%	0.5%	0.3%

Table 5: Model Scale Wave Cases for the Surf-Riding/Broaching-to Simulations

Wave Case	Wave Length (m)
1	5.290
2	6.795
3	8.489
4	10.369

The roll and yaw angles for each wave cases are plotted in Fig. 19 through to Fig. 22. From these figures it can be confirmed that the roll and yaw angles are strongly dependent on each other. The yaw angle remains relatively constant for the first three seconds and then over a period of approximately five seconds vessel yaws significantly by over 15 degrees. According to Spyrou [29], a yaw angle that exceeds 10 degrees can be denoted as a broach. Therefore, under these circumstances the OPV will broach when subjected to each of the

aforementioned wave cases. It was observed that when the waves would crash over the stern deck of the vessel the free surface moment created by the wave could have exacerbated the roll behaviour of the vessel. Although this cannot be confirmed and should be investigated further. However, the free surface effect created by the waves can be visually seen in Fig. 8. Operational guidance for the vessel can begin to be developed for the vessel using results found. Once the vessels behaviour has been investigated over a series of wavelength, wave heights, and wave encounter angle the information could be used to support the “Guidance to the Master for Avoiding Dangerous Situations in Adverse Weather and Sea Conditions” [30]. The results presented were found to be within the at risk zone stipulated in MSC1/Circ.1228 [30].

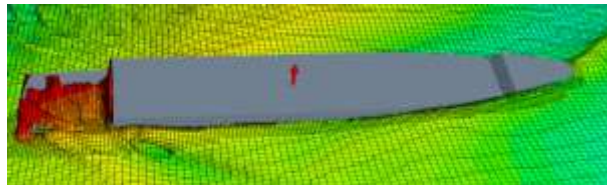


Fig. 8: Star CCM+ Image of the Heeled OPV with a Wet Aft Deck; Wavelength = 10.4m

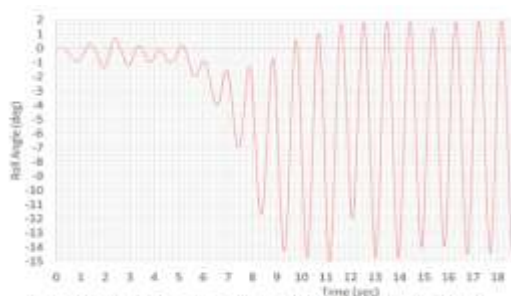


Fig. 19: Amplification of the Roll Angle for the OPV; Wavelength = 5.3m

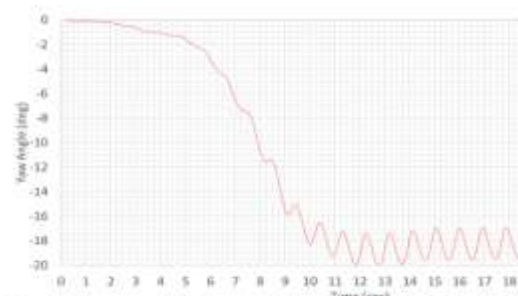


Fig. 20: Exponential Increase of the Yaw Angle of the OPV; Wavelength = 5.3m

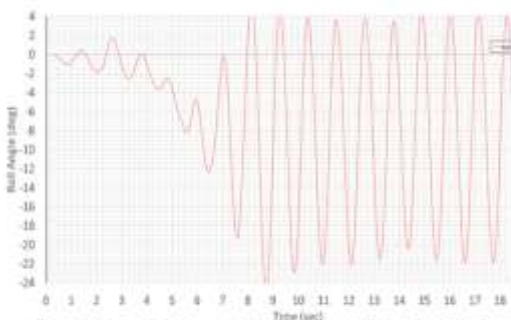


Fig. 21: Amplification of the Roll Angle for the OPV; Wavelength = 6.8m



Fig. 22: Exponential Increase of the Yaw Angle of the OPV; Wavelength = 6.8m

V. CONCLUSION

The draft SGISC has been applied to the NZ OPV and evaluated. It was determined that the OPV, without appendages, was found to be vulnerable at level one for the pure loss of stability and surf-riding/broaching-to criteria, with the vessel failing the level two vulnerability assessment for surf-riding/broaching-to in certain operationally avoidable operational encounter conditions.

A computational analysis has been conducted to determine the vulnerability of a NZ Navy OPV hull form to the surf-riding/broaching-to phenomenon. The analysis was conducted using the RANS solver STAR CCM+ using first order VOF waves over a series of wavelengths.

It was found that the resistance extrapolation method recommend by China, is not ideal. Ideally, it is recommended that when determining the resistance curve for the level two surf-riding/broaching-to criterion to calculate the resistance for the vessel from low Froude numbers, approximately $F_N=0.1$, up to 0.7 and fitting a five power polynomial curve. However, when this cannot be completed, effort should be made to determine the resistance for the vessel within the Froude number range of 0.399 to 0.691.

The 5 power polynomial resistance equation of the NZ OPV introduced a constant error of 13% compared to the actual CFX simulation results.

Further Work

The OPV has not been tested to the other SGISC level two criteria. These should be applied to ensure no false negatives occur. A selection of other vessels should also be applied to the SGISC to produce a range of results to compare common traits in vulnerabilities. The direct assessment has not been validated with scaled model testing. The model OPV hull form analysed should be constructed at and be tested experimentally, in the towing tank, in order to verify that the simulation accuracy is correct. Further direct assessment simulations should be conducted with the appendages attached to show how the appendages influence the hull forms behaviour. A surging simulation should be investigated to determine the surf-riding characteristics of the hull form. This can then be used to compare and contrast the broaching-to simulation conducted and determine whether the determined results are pessimistic or valid. The influence of twin rudders, and bilge keels, is suspected to improve directional stability in a surf-riding/ broaching scenario. The likely affect on trim may also be of interest to investigate further. It is also possible that a vessel trimming by the bow could an increased broaching susceptibility.

The relationship between the wave length and roll angle should be investigated further and compared to the summation of the steady roll angle and the roll angle determined for the vessel with zero velocity. The simulation conducted used a stationary model. Because of this condition, the roll angle due to turning has not been accounted for. With the further assumption that the vessel is steady, i.e. the accelerations are zero, and the centre of lateral resistance is level with the centre of buoyancy, the steady heel angle in a turn can be determined by Lewis [31]. Where the non-dimensional equations of moment can be determined using the Clarke coefficients [32]. Assuming that the vessel moves at the same velocity as the wave [26], the heel angle in a turn, relative to the wavelength, can be determined. Although the steady heel angle calculation is not a correct representation of broaching behaviour, the angle calculated can be used as an approximation for the expected roll angle experienced when the vessel broaches.

Operational guidance for the vessel should be established by investigating the vessels behaviour over a series of wavelengths, wave heights, and wave encounter angles to determine whether the vessel is vulnerable. Until the draft criteria are finalised and operational guidance is provided, the IMO MSC guidance identifies the susceptible region for surf-riding and broaching-to and should be the first point of reference.

REFERENCES

- [1]. Peters, W., Belenky, V., Bassler, C., Spyrou, K., Umeda, N., Bulian, G., & Altmayer, B. (2011). The second generation of intact stability criteria: an overview of development. Paper presented at the SN AME Annual Meeting and Expo, Houston, TX.
- [2]. Kure, K., & Bang, C. (1975). The ultimate half roll. Paper presented at the International Conference on Stability, Glasgow.
- [3]. France, W. N., Levadou, M., Treacle, T. W., Paulling, J. R., Michel, R. K., & Moore, C. (2003). An investigation of head-sea parametric rolling and its influence on container lashing systems. *Marine Technology*, 40(1), 1-19.
- [4]. Pérez Rojas, L., Sastre, S., & Martín Landaluce, A. (2008). Review of the ship accidents investigations presented at the STAB.
- [5]. SLF53. (2011). Report to the Maritime Safety Committee.
- [6]. Bassler, C. C., Belenky, V., Bulian, G., Francescutto, A., Spyrou, K., & Umeda, N. (2011). Review of available methods for application to second level vulnerability criteria. *Contemporary Ideas on Ship Stability and Capsizing in Waves*, 3-23.
- [7]. Belenky, V., Bassler, C. G., & Spyrou, K. J. (2011). Development of Second Generation Intact Stability Criteria.
- [8]. Spyrou, K. (2000). Designing against parametric instability in following seas. *Ocean Engineering*, 27(6), 625-653.
- [9]. Tuite, A. (1997). Broaching: An extreme nonlinear motion Experienced by small vessels in astern seas. Doctoral Thesis ,Australian Maritime College ,Tasmania, Australia.
- [10]. Umeda, N., Hashimoto, H., Vassalos, D., Urano, S., & Okou, K. (2004). Nonlinear dynamics on parametric roll resonance with realistic numerical modelling. *International shipbuilding progress*, 51(2, 3), 205-220.
- [11]. Jordan, D. W., & Smith, P. (2007). *Nonlinear ordinary differential equations*: Oxford Univ. Press.
- [12]. Belenky, V., de Kat, J. O., & Umeda, N. (2008). Toward performance-based criteria for intact stability. *Marine Technology*, 45(2), 101-120.
- [13]. Belenky, V. L., & Sevastianov, N. B. (2007). *Stability and safety of ships: risk of capsizing*.

- [14]. Spyrou, K. (1996). Dynamic instability in quartering seas: the behavior of a ship during broaching. *Journal of Ship Research*, 40(1), 46-59.
- [15]. Spyrou, K. (2006). Asymmetric surging of ships in following seas and its repercussions for safety. *Nonlinear Dynamics*, 43(1-2), 149-172.
- [16]. Umeda, N. (2013). Current Status of Second Generation Intact Stability Criteria Development and Some Recent Efforts. Paper presented at the Proceedings of the 13th Int. Ship Stability Workshop Brest.
- [17]. CD-Adapco, S.-C. (2014). v. 10 Help manual.
- [18]. BentleySystems. (2016). Maxsurf Resistance Manual.
- [19]. BentleySystems. (2016). Maxsurf Motions Manual.
- [20]. Biran, A., & Pulido, R. L. (2013). *Ship hydrostatics and stability*: Butterworth-Heinemann.
- [21]. IMO. (2008). *International Code on Intact Stability*. (London: International Maritime Organization).
- [22]. Balcer, L. (2004). Location of ship rolling axis. *Polish Maritime Research*(1), 3-7.
- [23]. Molland, A. F., Turnock, S. R., & Hudson, D. A. (2011). *Ship resistance and propulsion: practical estimation of propulsive power*: Cambridge university press.
- [24]. John, S., Khan, K., Praveen, P., Korulla, M., & Panigrahi, P. (2012). Ship Hull Appendages: A Case Study. *International Journal of Innovative Research and Development*, 1(10), 74-89.
- [25]. Haase (2016, Personal Communication, 27 May 2016.
- [26]. Belenky, V., Spyrou, K., Weems, K., (2011). Split-time method for surf-riding and broaching-to. Paper presented at the Proceedings, 12th International Ship Stability Workshop, Washington DC. June.
- [27]. SDC3/6/6. (2015). Finalization of Second-Generation Intact Stability Criteria Submitted by China.
- [28]. ITTC. (2011). *Practical guidelines for ship CFD Applications., Recommendations and Procedures*.
- [29]. Spyrou, K. (1997). Dynamic instability in quartering seas-Part III: Nonlinear effects on periodic motions. *Journal of Ship Research*, 41(3), 210-223.
- [30]. MSC. (2007). 1/Circ. 1228 Revised guidance to the Master for avoiding dangerous situations in adverse weather and sea conditions. International Maritime Organization (IMO), London, UK.
- [31]. Lewis, E. V. (1988). *Principles of Naval Architecture: Motions in waves and controllability (Vol. 3)*: Society of Naval Architects and Marine Engineers.
- [32]. Clarke, D., Gedling, F., & Hine, G. (1982). The application of maneuvering criteria in hull design using linear theory. *The Royal Institution of Naval Architects*, 45-68.